processes

MDPI

Article

Performance Degradation Modeling and Continuous Worktime Assessment of Ultrasonic Vibration Systems

Ruoyu Wang, Lei You and Xiaoping Hu *

School of Mechanical Engineering, Hangzhou Dianzi University, Hangzhou 310018, China; wangruoyu@hdu.edu.cn (R.W.)
* Correspondence: xiaoping.hu@hdu.edu.cn

Abstract: In order to assess the stable operating duration of an ultrasonic vibration system, a reliability-based analysis method for the stability of the ultrasonic vibration system is proposed. Firstly, the failure mechanisms of the ultrasonic vibration system are analyzed, and the resonant frequency and amplitude are selected as two degradation features of the system. Subsequently, accelerated degradation experiments under different force loads were conducted, and the degradation model of the ultrasonic vibration system was established by comparing experimental data with degradation, distribution, and acceleration models. Finally, Copula functions were introduced to connect the two degradation features, resonant frequency, and amplitude, and lifetime curves were plotted under the influence of univariate and bivariate degradation factors. Through the analysis of the lifetime curves, the conclusion is drawn that the decay of amplitude is the primary indicator of system lifetime, and it is predicted that the developed ultrasonic vibration system can operate continuously and stably for 26.69 h. This research is of great significance for enhancing the reliability and lifespan management of ultrasonic vibration systems.

Keywords: ultrasonic vibration system; reliability theory; degradation model; copula function; lifetime prediction

Citation: Wang, R.; You, L.; Hu, X. Performance Degradation Modeling and Continuous Worktime Assessment of Ultrasonic Vibration Systems. *Processes* **2024**, *12*, 439. https://doi.org/10.3390/pr12030439

Academic Editors: Hongyun So, Jong-Won Park and Sunghan Kim

Received: 31 January 2024
Revised: 12 February 2024
Accepted: 18 February 2024
Published: 21 February 2024

1. Introduction

With the continuous development of industrial technology, ultrasonic processing technology has been widely applied in material processing due to its advantages of a low cutting force, high processing efficiency, and environmental friendliness [1]. In the process of ultrasonic cutting, it is essential for the ultrasonic vibration system to work continuously, without faults, and stably to ensure the quality of the processing. However, research has shown that the ultrasonic system can experience phenomena such as frequency drift and amplitude decay during processing due to external loads, which can impact the stability and the quality of ultrasonic cutting. Currently, there are no standardized regulations for evaluating the continuous and stable operation of ultrasonic systems, and there is a lack of corresponding experimental test data. Reliability studies utilize the degradation characteristics of a system to assess its reliability, providing a new approach for studying the continuous operational lifespan of ultrasonic systems.

Research on the working characteristics of ultrasonic vibration systems has been limited both domestically and internationally. Zhou H et al. [2] proposed an output amplitude model that takes into account the effects of loading, exploring how loading affects the amplitude stability of ultrasonic vibration systems. Zhao B et al. [3], through variable load experiments, concluded that mechanical loading can impact the resonant frequency and amplitude output of the system. Chenjun W et al. [4] established a dynamic model for ultrasonic vibration milling based on mechanical vibration and the longitudinal torsion theory and used a modified semi-discrete approach to describe its stability. However, they did not study the degradation process of ultrasonic vibration systems under loading.

For general systems, Dong X et al. [5] combined Weibull distribution with the hazard ratio to construct a prediction model and predicted the lifespan of electricity meters. Park M et al. [6] conducted accelerated lifespan tests on railway vehicle contactors by applying high stress, determining the failure modes of the contactors, and evaluating their lifespan. Nevertheless, during the process of modeling system performance degradation, there may be various coexisting failure characteristics, leading to the introduction of Copula functions. Fang G et al. [7] studied a coherent system with positively correlated performance degradation processes and proposed a flexible bivariate stochastic process considering the influence of environmental stress variables to analyze accelerated degradation data, modeling the correlation between the two degradation processes using Copula functions. Sun F et al. [8] described the degradation of characteristics using Brownian motion for products with multiple performance degradation features and established a time-varying Copula function to address reliability assessment issues for such products.

In recent years, the modeling of performance degradation has become the mainstream approach for predicting product lifespan. This paper focuses on the ultrasonic cutting processing system as the research subject. It analyzes and selects two failure assessment features, namely resonant frequency drift and amplitude decay, to reflect the entire system's degradation process. It explores the degradation models of ultrasonic vibration systems under the influence of single failure features and dual failure features. This enables the assessment of the lifespan of ultrasonic vibration systems operating continuously and stably. The research provides a reference basis for practical production applications of ultrasonic processing.

2. Ultrasonic Machining Systems and Failure Analysis

2.1. Introduction to Ultrasonic Machining Systems

The ultrasonic machining system consists of an ultrasonic power source and an ultrasonic vibration system. The ultrasonic vibration system is primarily composed of a transducer, an amplitude modulator, and a machining tool. The ultrasonic power source converts low-frequency AC power at 50 Hz into ultrasonic frequencies of 20 kHz and above, supplying them to the ultrasonic vibration system while continuously tracking the resonant frequency of the vibration system. Transducers are generally of the piezoelectric type, utilizing the inverse piezoelectric effect of piezoelectric elements to transform the electrical signals from the power source into mechanical vibration signals. These signals are then amplified by the amplitude modulator and ultimately transmitted to the machining tool to facilitate ultrasonic material processing. Figure 1 shows a schematic diagram of the ultrasonic vibration system processing a Nomex honeycomb composite material.

2.2. Failure Analysis of Ultrasonic Vibration Systems

The types of failures in electromechanical systems are typically categorized based on failure mechanisms as sudden and degradation types. Sudden failure refers to a situation where the system abruptly transitions from normal operation to a state where it can no longer function. In contrast, degradation-type failures involve the gradual deterioration of certain performance parameters within a normally functioning system over time, ultimately reaching the system's failure criteria. Ultrasonic vibration systems, as typical examples of electromechanical integrated systems, have relatively few instances of sudden failure and are more commonly associated with degradation-type failures.

Drawing on the research conducted by our research group on the development and engineering application of ultrasonic machining systems [3,9], we chose to focus on the ultrasonic cutting of aerospace Nomex honeycomb composite materials. Initially, ultrasonic vibration systems are typically designed under no-load conditions. However, in practical working conditions, the influence of machining loads can alter the system's resonant frequency. When the resonance frequency shifts beyond the tracking range of the ultrasonic power source, typically within $\pm$200 Hz, the resonance frequency no longer matches the power source's output frequency, rendering the entire system unable to resonate and main-

tain stable machining conditions. Additionally, due to the continuous impact of machining loads, the ultrasonic power source must output higher power to accommodate, leading to an increase in the working temperature of the piezoelectric transducer. This rise in temperature can result in delamination between the piezoelectric material layer and the electrode layer, reducing the electromechanical coupling performance. As a result, the efficiency of ultrasonic energy transmission decreases, and the amplitude output at the tool end diminishes, occasionally leading to cessation of vibration. When the amplitude decreases to below 10 μm, cutting the material becomes notably challenging, causing a decline in the quality of the workpiece. Given these factors, the analysis of ultrasonic vibration system failures selected resonant frequency drift and amplitude as degradation characteristics.

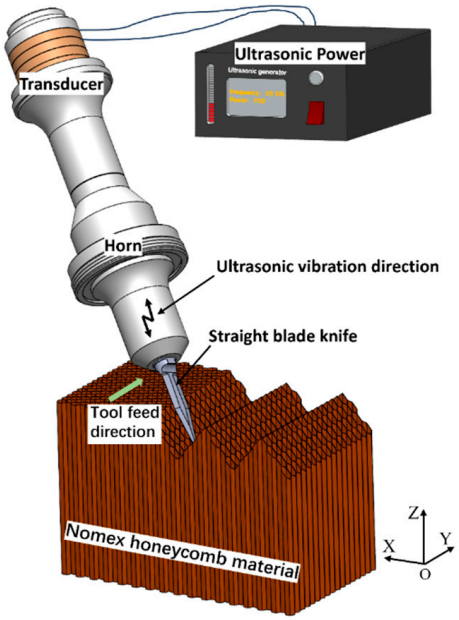

Figure 1. Nomex honeycomb material ultrasonic machining system.

Currently, there are no unified standards for evaluating the failure of ultrasonic vibration systems, both domestically and internationally. Based on the analysis mentioned above, the criteria for ultrasonic vibration system failure have been established as drift in the working resonant frequency exceeding ±200 Hz and an output amplitude decreasing to below 10 μm. Considering that the predominant form of cutting load in ultrasonic machining of honeycomb composite materials is in the form of cutting forces, cutting forces are identified as the primary cause of failure in ultrasonic vibration systems.

3. Ultrasonic Vibration System Accelerated Degradation Model

3.1. Degradation Modeling Process

Products with degradation-type failures can use degradation modeling to describe their degradation process. By applying the concept of accelerated degradation, an ultrasonic machining system degradation model can be established. The steps of the statistical modeling process for reliability are depicted in Figure 2. Based on the system's working load conditions and its tolerance levels, suitable stress levels and corresponding experimental times are designed. Degradation data are then fitted through degradation modeling and distribution modeling to obtain a distribution model of pseudo-failure lifespan under accelerated degradation. Subsequently, a mathematical relationship between the parameters in the distribution model and the external stress is established to create an acceleration model. This transformation allows for the conversion of distribution parameters from high-stress levels to normal stress levels, thereby completing the entire degradation modeling of the system.

Figure 2. Reliability statistical modeling process.

3.2. Accelerated Experiments and Data Collection

Accelerated experiments are a method for subjecting a product to load conditions higher than those encountered under normal operating conditions to collect additional system degradation parameters [10]. Accelerated experiments can be divided into accelerated lifespan experiments and accelerated degradation experiments. Accelerated degradation experiments are less time consuming and cost effective compared to the former. The fundamental assumption is that the performance degradation trend in the system under accelerated conditions is the same as that under normal conditions, and the failure mechanism of the system under accelerated conditions remains unchanged. The performance degradation process of the ultrasonic machining system meets the basic assumptions of accelerated degradation experiments. Therefore, it is reasonable to control the range of accelerated stress for accelerated degradation experiments. This study uses a constant stress level for accelerated degradation experiments to simplify the computational process.

According to national standards, the minimum number of stress levels for accelerated experiments should be at least three, with the lowest stress level being greater than the normal operating stress value. The highest stress level should be as high as possible within the stress range that the product can physically withstand. In normal cutting of honeycomb materials, the ultrasonic vibration system is mainly subjected to the cutting force in the feed direction, and the maximum range of the normal cutting force load is within 20 N [11]. Due to experimental limitations, the cutting force is considered as a constant force load, and a tension–compression force gauge is used to simulate the primary cutting force acting on the tool during the cutting process. When the cutting force increases to 40 N, the experiment shows that the dynamic resistance of the ultrasonic vibration system is close to 110 Ω [12], and changes in dynamic resistance can affect the system's matching performance. Therefore, to minimize the impact on the system, three sets of experimental stress levels are designed as follows: $S_1 = 25$ N, $S_2 = 30$ N, $S_3 = 35$ N.

The experimental setup is shown in Figure 3, with a self-developed ultrasonic vibration system with a resonant frequency of approximately 20 kHz. The ultrasonic generator uses a Mingquan MQ-2000 anti-resonant frequency electronic signal generator, which has automatic frequency tracking capabilities. The ultrasonic generator generates an AC electrical signal of 20 kHz, which is then transmitted to the piezoelectric element of the ultrasonic vibration system's transducer. Through the piezoelectric effect, the electrical signal is converted into mechanical vibrations, thereby generating small ultrasonic vibrations. These vibrations are then amplified by an amplitude modulator and transmitted to the tool head to generate high-frequency vibrations. The ultrasonic tool, developed in-house, is made of high-speed steel and has a length of 37 mm. To determine the ultrasonic amplitude of the tool, a Keyence LK-G5000 laser displacement sensor is used, with a sampling rate of 392 kHz and an accuracy of ±0.02%. To simulate the cutting force load during ultrasonic vibration cutting, an HP-100 digital tension–compression force gauge is used, with a resolution of 0.01 N, an accuracy of ±1%, and a maximum load capacity of 100 N. The tension–compression load cell is applied to the cutting edge, and a honeycomb-like material is inserted between the load cell probe and the tool to simulate real cutting of honeycomb material. The slide table can be adjusted as needed to obtain different cutting forces. The frequency acquisition module uses an Advantech ADAM-5081.

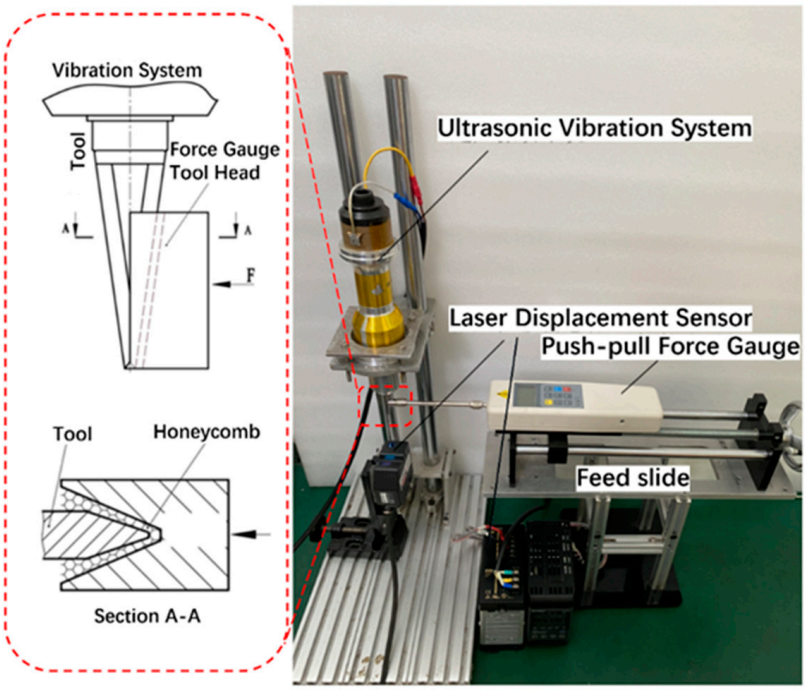

Figure 3. Ultrasonic cutting force load experimental platform.

Following the above design, experiments were conducted, and to enhance experimental accuracy, data from five samples were collected for each stress level. Figure 4 displays the median values and error bands for each sample group.

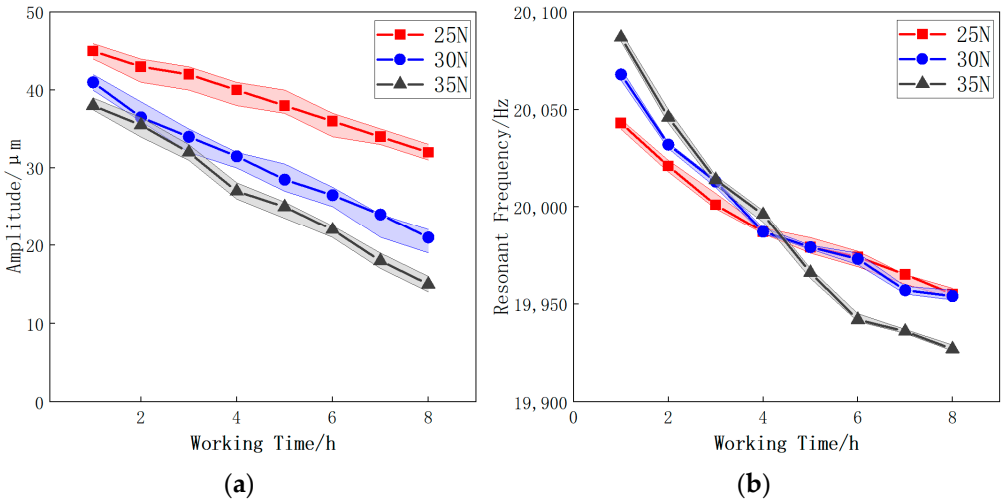

Figure 4. Degradation data graph of feature quantity with working time. (**a**) Resonant frequency degradation diagram; (**b**) Amplitude degradation diagram.

As shown in Figure 4, under the influence of the force load, both degradation characteristics, namely resonant frequency and amplitude, exhibit a decline. Furthermore, as the force load increases, the degradation of these amplitude and resonant frequency characteristics becomes more pronounced.

3.3. Establishment of the Degradation Model

A degradation model is a mathematical function expression established using mathematical statistical methods to describe the relationship between degradation and time. Commonly used degradation fitting models include linear models, exponential models,

Weibull models, power law models, and others [13]. Using the CFTOOL tool in Matlab, least-squares fitting is performed separately on the degradation trajectories of resonant frequency and amplitude at different stress levels. Figure 5 displays the fitted curve for the degradation trajectory of resonant frequency at 25 N stress.

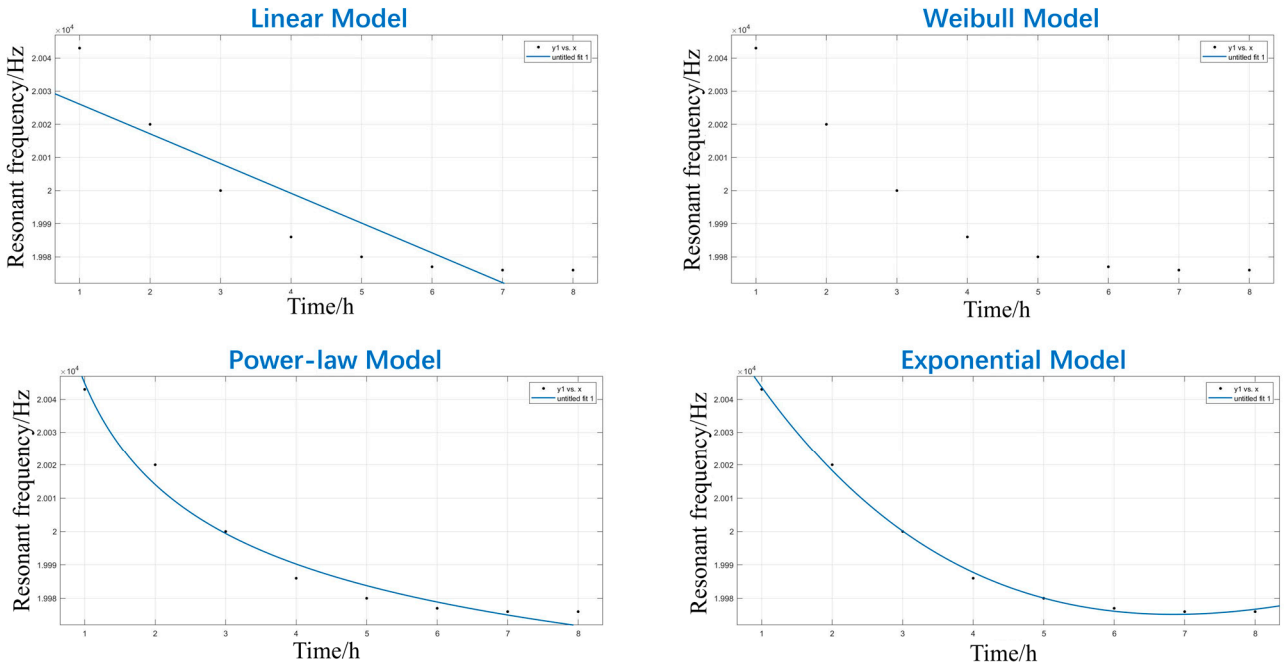

Figure 5. Fitting curve of resonant frequency degradation trajectory under 25 N stress.

Similarly, the degradation trajectories of resonant frequency at stress levels of 30 N and 35 N, as well as the degradation trajectories of amplitude at different stress levels, were fitted. From Figure 5, it is evident that the linear model and Weibull model have poor fitting effects, while the Power-law model and Exponential model have better fitting effects. It is necessary to evaluate the fitting degree of these two models; therefore, the complex correlation coefficient R^2 was introduced [14]:

$$R^2 = 1 - \frac{SSE}{SST} \tag{1}$$

where SSE represents the sum of squared residuals, and SST represents the total sum of squares. The calculated results are presented in Table 1.

Table 1. R-squared value with resonance frequency as the degradation factor.

Fitting Model	Linear Model		Weibull Model		Power-Law Model		Exponential Model	
Degenerative Features	Resonant Frequency	Amplitude	Resonant Frequency	Amplitude	Resonant Frequency	Amplitude	Resonant Frequency	Amplitude
25 N	0.9636	0.9859	-4.5×10^5	−77.95	0.9805	0.8461	0.9974	0.9806
30 N	0.9215	0.9946	-2.9×10^5	−20.68	0.9926	0.8835	0.9943	0.9892
35 N	0.9550	0.9961	-1.4×10^5	−8.895	0.9831	0.8231	0.9954	0.9742

R^2 is an indicator used to assess the goodness of fit between independent and dependent variables. Its values range from 0 to 1, with values closer to 1 indicating a higher degree of fit. If the value is negative, it suggests significant deviations. Based on the R^2 test results in Table 1, the conclusion can be drawn that the degradation trajectories of the resonant frequency and amplitude in the ultrasonic vibration system are best fitted using an

exponential model and a linear model, respectively. Thus, the equations for the degradation trajectories of resonant frequency and amplitude can be expressed as Equation (2) and Equation (3), respectively [14]:

$$y_1 = a \cdot e^{bx} + c \cdot e^{dx} \quad (2)$$

$$y_2 = a_1 x + b_1 \quad (3)$$

The parameters a, b, c, d in the exponential model, and the parameters a_1 and b_1 in the linear model can be obtained through fitting using the least-squares principle within the CFTOOL toolbox. By substituting the failure thresholds for resonant frequency and amplitude into their respective performance degradation trajectory equations, the pseudo-failure lifespans of the ultrasonic vibration system at different load levels can be calculated, as shown in Table 2.

Table 2. Pseudo-failure lifespans under different failure factors.

Stress Level	**S_1 = 25 N**		**S_2 = 30 N**		**S_3 = 35 N**	
Degenerative Features	**Resonant Frequency**	**Amplitude**	**Resonant Frequency**	**Amplitude**	**Resonant Frequency**	**Amplitude**
Sample 1	25.1 h	19.7 h	20.7 h	12.1 h	13.9 h	9.2 h
Sample 2	31.7 h	20.5 h	23.5 h	11.9 h	13.2 h	9.8 h
Sample 3	24.4 h	20.5 h	17.5 h	10.8 h	13.4 h	9.3 h
Sample 4	24.0 h	20.7 h	18.1 h	11.9 h	13.6 h	9.1 h
Sample 5	26.5 h	19.8 h	18.4 h	12.5 h	12.9 h	9.5 h

3.4. Establishment of the Distribution Model

When conducting each set of degradation experiments, multiple sample data points are typically collected. The lifespans of these samples can exhibit variations, and understanding the distribution that the sample lifespans follow using an appropriate distribution model can enhance the reliability of the experiments. Commonly used distribution functions for electromechanical products include the log-normal distribution, Weibull distribution, normal distribution, and exponential distribution [15]. Using Minitab 20 data analysis software, a test was conducted on the pseudo-failure distribution of resonant frequency at the $S_1 = 25$ N stress level from Table 1, as shown in Figure 6, the red line represents the 95% confidence interval of each distribution, and the blue dots represent the data points.

From the graph, it can be seen that the data points for the normal distribution, log-normal distribution, and Weibull distribution are all within the 95% confidence interval, while the data points for the exponential distribution are not entirely within the 95% confidence interval. Therefore, it can be concluded that the resonant frequency does not follow an exponential distribution.

Likewise, hypothesis tests were performed on the distributions at other stress levels, and probability plots were created. The p-value was introduced for hypothesis testing, and in the hypothesis testing process, the p-value is the standard for significance testing. The larger the p-value, the closer it is to the null hypothesis. The calculated p-values are presented in Table 3.

Table 3. The p-values of each group distribution (with resonance frequency as the degradation factor).

Stress Level	**Normal**	**Lognormal**	**Weibull**	**Exponential**
25 N	0.084	0.119	0.081	0.007
30 N	0.228	0.280	0.223	0.008
35 N	0.946	0.946	>0.25	0.003

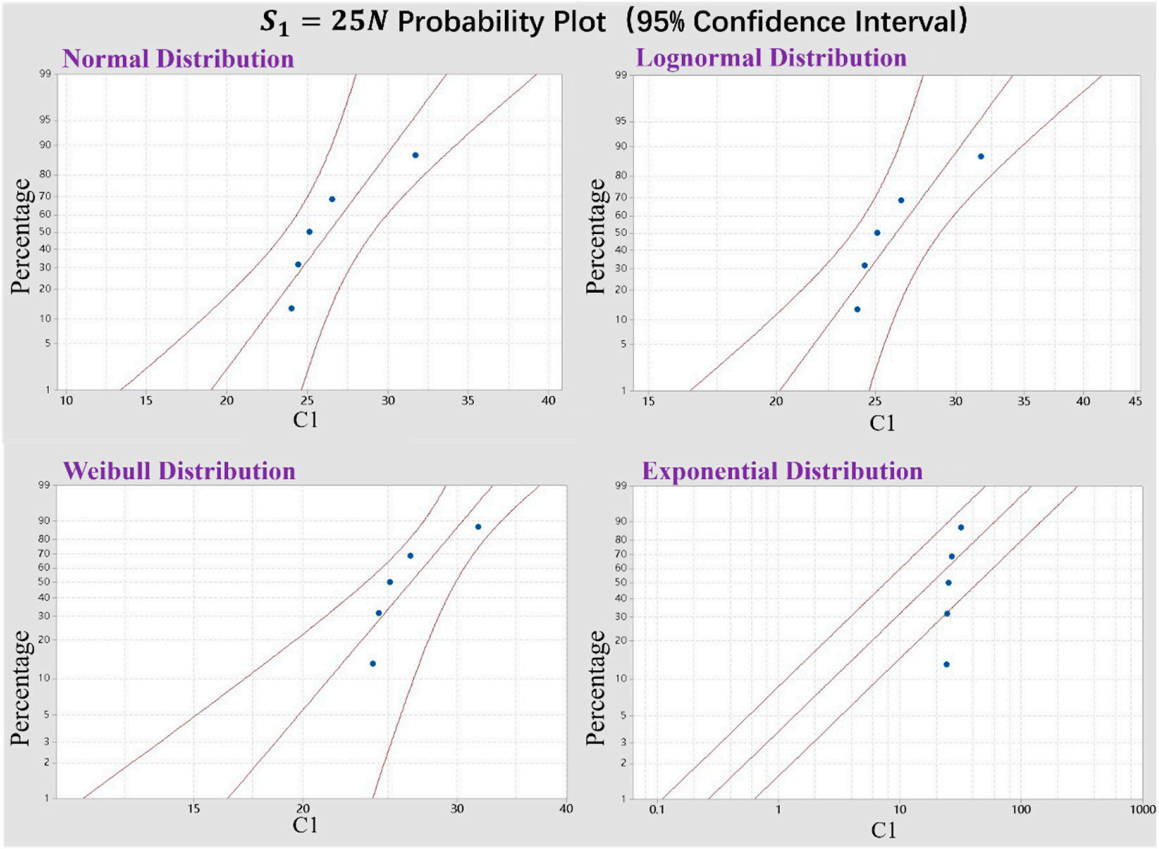

Figure 6. Probability plot of various distribution assumptions under 25 N stress.

From Table 3, it can be concluded that the pseudo-failure lifespan of the ultrasonic vibration system, with resonant frequency as the degradation metric, is better represented by a log-normal distribution. The corresponding probability density function $F(t)$ and reliability function $R(t)$ are as shown in Equations (4) and (5) [16]:

$$F_1(t) = \frac{1}{\sigma t\sqrt{2\pi}} exp\left[-\frac{1}{2}\frac{(lnt-\mu)^2}{\sigma^2}\right] \tag{4}$$

$$R_1(t) = \int_t^{\infty} \frac{1}{\sigma t\sqrt{2\pi}} exp\left[-\frac{1}{2}\frac{(lnt-\mu)^2}{\sigma^2}\right] \mathrm{dt}, t > 0 \tag{5}$$

Here, the parameters μ and σ^2 represent the mean and variance of the log-normal distribution, respectively.

Using a similar analytical approach, it can be determined that the pseudo-failure lifespan of the ultrasonic vibration system, with amplitude as the degradation metric, is better represented by a Weibull distribution. The corresponding probability density function $F(t)$ and reliability function $R(t)$ are as shown in Equations (6) and (7) [16]:

$$F_2(t) = \frac{\beta}{\eta}\left(\frac{t}{\eta}\right)^{\beta-1} exp\left[-\left(\frac{t}{\eta}\right)^{\beta}\right] \tag{6}$$

$$R_2(t) = exp\left[-\left(\frac{t}{\eta}\right)^{\beta}\right], t > 0 \tag{7}$$

In these equations, β represents the shape parameter and η represents the scale parameter.

The parameters obtained from the fitting for both the log-normal and Weibull distributions are presented in Table 4.

Table 4. Parameters of log-normal distribution and Weibull distribution.

Stress		25 N	30 N	35 N
Lognormal Distribution	μ	3.226	2.972	2.595
	σ	0.113	0.1215	0.0284
Weibull Distribution	β	61.7	29.9	37.09
	η	20.42	12.08	9.521

3.5. Establishment of the Acceleration Model

The acceleration model is used to transform the distribution model parameters corresponding to high-stress levels into distribution parameters under normal stress conditions. Currently, widely applicable acceleration models include Arrhenius, Inverse Power Law, Eyring, Polynomial acceleration models, and more. The relationship between the degradation rates under mechanical stress and stress is often described using the Inverse Power-law model, obtained from a large number of physical experimental data [8]:

$$\mathrm{K} = \mathrm{AS}^{-\mathrm{c}} \tag{8}$$

where K is the degradation rate in the degradation process, S represents the stress level, and A and c are constants. The linear inverse Power-law model can be obtained by taking the logarithm of both sides of the equation:

$$\ln\ \mathrm{K} = \ln\mathrm{A} - \mathrm{c} \cdot \ln\ \mathrm{S} \tag{9}$$

Combining the parameter values from Table 4, the Inverse Power-law model for the normal distribution and Weibull distribution is given by Equations (10) and (11):

$$\begin{cases} \mu = 9.242 - 1.816 \times lnS \\ \sigma = 0.9099 - 0.2424 \times \ln S \end{cases} \tag{10}$$

$$\begin{cases} \beta = 301.3 - 76.2 \times \ln S \\ \eta = 125.2 - 32.79 \times \ln S \end{cases} \tag{11}$$

4. Ultrasonic Machining System Lifetime Assessment

4.1. Univariate Reliability Modeling

For the ultrasonic vibration system with resonant frequency as the degradation metric, the pseudo-failure lifespan follows a normal distribution. By substituting the normal cutting force S = 20 N into the Inverse Power Law model in Equation (10), the distribution parameters for the ultrasonic vibration system under normal stress conditions are obtained as: μ = 3.892, σ = 0.1849. For the ultrasonic vibration system with amplitude as the degradation metric, the pseudo-failure lifespan follows a Weibull distribution. By substituting the normal cutting force S = 20 N into the Inverse Power-law model in Equation (11), the distribution parameters for the ultrasonic vibration system under normal stress conditions are obtained as: β = 73, η = 27.

By plugging these distribution parameters into Equations (5) and (7), the reliability functions $R_1(t)$ and $R_2(t)$ are obtained. These reliability functions, derived from a single degradation metric, represent the working lifespan of the system influenced by a single degradation metric, as shown by the black square curve and brown dashed curve in Figure 7.

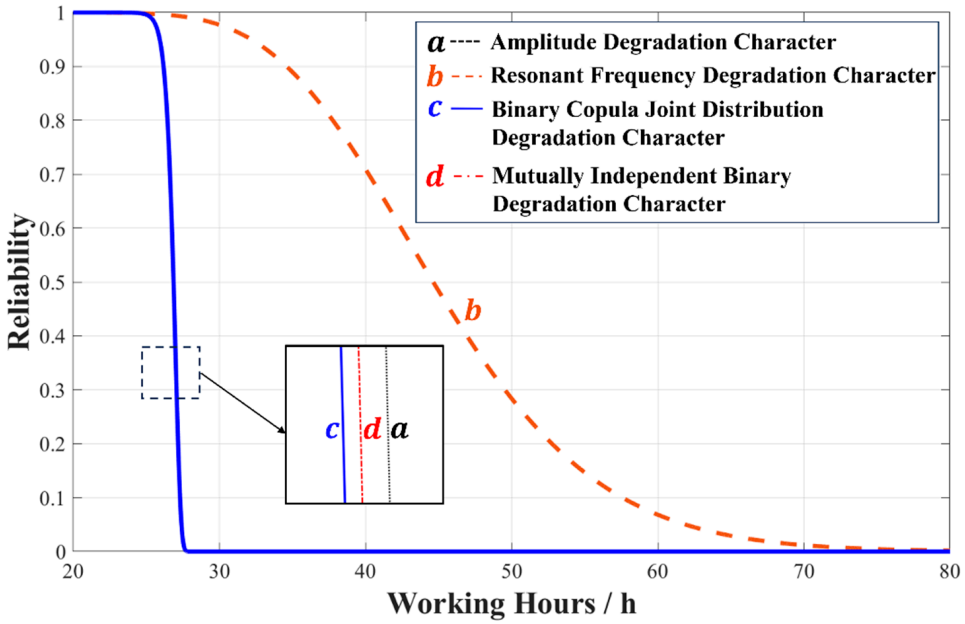

Figure 7. Reliability curve comparative graph.

4.2. Bivariate Reliability Modeling

4.2.1. Modeling with Two Independent Degradation Features

In practice, the ultrasonic vibration system may be influenced by multiple degradation features simultaneously. If there is no correlation between these degradation features, according to reliability theory, the total reliability function $R'(t)$ of the system is the product of the reliability functions under the distributions of each degradation feature, i.e.,

$$R'(t) = R_1(t) \cdot R_2(t) \tag{12}$$

A bivariate reliability curve can be plotted for the ultrasonic machining system where two independent degradation modes affect the system, as shown by the red dashed line curve in Figure 7.

4.2.2. Modeling with Two Correlated Degradation Features

If there is a correlation between the different degradation features of the system; Copula functions can be used as connecting functions. Copula functions can connect the marginal distribution functions corresponding to amplitude and resonant frequency, effectively solving the problem of complex correlations under multiple degradation modes. There may be a certain correlation between the degradation of amplitude and resonance frequency, which jointly affect the performance of the ultrasonic vibration system. This helps in establishing the joint distribution reliability function $R''(t)$ for the ultrasonic vibration system under the influence of different degradation features together.

Copula functions are commonly used to describe the correlation between multiple random variables. Assuming there are n-dimensional random variables X_1, X_2, $\cdots$, X_n with correlations among them, and there is a Copula function $C(u_1, u_2, \cdots, u_n)$ such that the marginal distribution functions of the random variables are $F_1(x_1)$, $F_2(x_2)$, $\cdots$, $F_n(x_n)$; the following expression holds between the joint distribution function $F(x_1, x_2, \cdots, x_n)$ and the Copula function [17]:

$$\begin{aligned} F(x_1, x_2, \ldots, x_n) &= C[F_1(x_1), F_2(x_2), \cdots, F_n(x_n); \theta] \\ &= C[F_i(x_i); \theta | i = 1, 2, \ldots, n] \end{aligned} \tag{13}$$

where θ is the parameter vector in the Copula function, and its value determines the strength of the correlation described by the Copula function among various random variables.

Commonly used families of Copula functions in research include Gaussian Copula, t-Copula, and Archimedean Copula. Among these, the Archimedean Copula family has a simpler structure, and its analytical expressions are clearer, making it widely applied. Some commonly used Archimedean Copula functions include the Frank Copula function, Clayton Copula function, and Gumbel Copula function [18].

The marginal distribution functions $u = F_1(t)$ and $v = F_2(t)$ for frequency and amplitude are used as input values in the Copula function. The Copula function parameters θ are then calculated using the maximum likelihood estimation method [19].

$$L(\theta) = \sum_{i=1}^{n} lnc(F_1(t), F_2(t); \theta) \tag{14}$$

By taking the derivative of the parameters θ in Equation (14) and setting the derivative to 0, the values of the Copula function parameters can be determined, as shown in Table 5.

Table 5. Parameter value θ of the copula function.

Copula Function	θ
Frank Copula	0.19629
Clayton Copula	0.08887
Gumbel Copula	1.10000

In order to assess the strength of different Copula functions in describing the correlation between different variables, the AIC, BIC, and DIC evaluation criteria were introduced to evaluate the Copula function models [20]. The model with the smallest value was chosen to describe the system's correlation, as shown in Table 6.

Table 6. AIC, BIC, DIC values.

Copula Function	AIC	BIC	DIC
Frank Copula	0.02026	0.04631	0.00013
Clayton Copula	0.01124	0.03730	−0.00438
Gumbel Copula	2.75826	2.78431	1.36913

After calculations, the Clayton Copula function model with the smallest value was chosen to describe the correlation between the two degradation features, resonant frequency, and amplitude. In this case, $\theta = 0.08887$.

Considering the overall reliability function $R''(t)$ for the ultrasound vibration system with the correlation between different failure characteristics, it can be expressed as [16]:

$$\begin{aligned} R''(t) &= P[F_1(t) \le D_1, F_1(t) \le D_2] \\ &= 1 - C[F_1(t), F_2(t)] \\ &= 1 - F_1(t) - F_2(t) + C(u, v; \theta) \\ &= R_1(t) + R_2(t) + C(u, v; \theta) - 1 \end{aligned} \tag{15}$$

where: D_1 and D_2 are the failure thresholds for the resonant frequency and amplitude, respectively, $C(u, v; \theta) = \left(u^{-\theta} + v^{-\theta} - 1\right)^{-\frac{1}{\theta}}$. The reliability function for the system with correlated degradation features, as depicted by the solid blue line in Figure 7, was generated using Matlab (R2018b) software.

Substituting $R(t) = 0.5$ into Equations (5), (7), (12), and (15), the median pseudo-failure time and the failure time for each group can be calculated, as shown in Table 7.

Table 7. System performance degradation time.

Degradation Character	Stable Working Time	Median Pseudo Failure Time	Failure Time
Resonant Frequency	23.86 h	49 h	86 h
Amplitude	25.15 h	27.01 h	28 h
Relevant	25 h	26.86 h	27.7 h
Independent	24.83 h	26.69 h	27.6 h

From Table 7 combined with Figure 7, it can be seen that:

(1) When considering resonance frequency as the degradation feature, the stable working time of the ultrasonic vibration system is 23.86 h, and the failure time reaches 86 h. This indicates that, even when the frequency tracking is good, the ultrasonic vibration system can maintain its operation for a longer period, even if it cannot maintain its initial optimal working state.
(2) When considering amplitude as the degradation feature, the stable working time and failure time are 25.15 h and 28 h, respectively, with only a 3 h difference between them. This suggests that amplitude degradation can rapidly lead to the failure of the system's operation.
(3) Whether considering only amplitude as the degradation feature or simultaneously considering both degradation features, the stable working time and failure time are roughly the same, ranging from 24.83 to 25.15 h and 27.6 to 28 h, respectively. The stable working time and failure time are both close to 3 h. This indicates that amplitude decay is the primary factor affecting the stable operation of the ultrasonic vibration system, making it more likely to cause the system's failure compared to frequency degradation.

5. Conclusions

During ultrasonic machining, the system's operational parameters degrade under the influence of applied mechanical loads. This paper investigates the degradation models of resonance frequency and amplitude of the ultrasonic machining system under different stress levels, with the main work and research findings summarized as follows:

(1) A detailed explanation of a degradation modeling approach for the ultrasonic vibration system is provided, encompassing the establishment of degradation models, distribution models, and acceleration models, which can serve as a reference for studies on the reliability of other complex systems.
(2) Based on accelerated degradation experiments and obtained degradation data, it is established that the exponential model works well to describe the drift in resonance frequency in the ultrasonic machining system under accelerated stress, while the linear model effectively represents the amplitude decay of the tool.
(3) Acceleration experiments were conducted on the developed ultrasonic vibration system under constant stresses of 25 N, 30 N, and 35 N. Considering the correlation between amplitude and resonance frequency, the conclusion drawn was that amplitude attenuation is the primary factor affecting the system's lifespan. The assessment indicated that, under normal conditions, the developed ultrasonic vibration system can work continuously and stably for a minimum of 26.69 h, providing a reference for practical applications in ultrasonic machining.

Author Contributions: Conceptualization, R.W., L.Y. and X.H.; methodology, R.W. and L.Y.; software, R.W.; validation, R.W., L.Y. and X.H.; formal analysis, L.Y.; investigation, R.W. and L.Y.; resources, L.Y.; data curation, L.Y.; writing—original draft preparation, R.W. and L.Y.; writing—review and editing, X.H.; visualization, R.W.; supervision, X.H.; project administration, R.W.; funding acquisition, X.H. All authors have read and agreed to the published version of the manuscript.

Funding: This research was funded by the National Natural Science Foundation of China (No. 51975173), Zhejiang Public Welfare Technology Research Program/Industry Project (Grant LGG21E050010).

Data Availability Statement: Data are contained within the article.

Conflicts of Interest: The authors declare no conflicts of interest.

References

1. Zhou, H.; Zhang, J.; Yu, D.; Wu, Z.; Cai, W. Advances in rotary ultrasonic machining system for hard and brittle materials. *Adv. Mech. Eng.* **2019**, *11*, 1687814019895929. [CrossRef]
2. Zhou, H.; Zhang, J.; Feng, P.; Yu, D.; Cai, W. An output amplitude model of a giant magneto strictive rotary ultrasonic machining system considering load effect. *Precis. Eng.* **2019**, *60*, 340–347. [CrossRef]
3. Zhao, B.; Bie, W.; Wang, X.; Chen, F.; Wang, Y.; Chang, B. The effects of thermo-mechanical load on the vibrational characteristics of ultrasonic vibration system. *Ultrasonics* **2019**, *98*, 7–14. [CrossRef] [PubMed]
4. Chenjun, W.; Shijin, C.; Kai, C.; Hui, D. Property study of power transmission system for rotary ultrasonic application. *Proc. Inst. Mech. Eng. Part C J. Mech. Eng. Sci.* **2018**, *232*, 305–315. [CrossRef]
5. Dong, X.; Jing, Z.; Dai, Y.; Wang, P.; Chen, Z. Failure Prediction and Replacement Strategies for Smart Electricity Meters Based on Field Failure Observation. *Sensors* **2022**, *22*, 9804. [CrossRef] [PubMed]
6. Park, M.; Rhee, S. A study on life evaluation & prediction of railway vehicle contactor based on accelerated life test data. *J. Mech. Sci. Technol.* **2018**, *32*, 4621–4628.
7. Fang, G.; Pan, R.; Hong, Y. Copula-based reliability analysis of degrading systems with dependent failures. *Reliab. Eng. Syst. Saf.* **2020**, *193*, 106618. [CrossRef]
8. Sun, F.; Wang, N.; Li, X.; Cheng, Y. A time-varying copula-based prognostics method for bivariate accelerated degradation testing. *J. Intell. Fuzzy Syst.* **2018**, *34*, 3707–3718. [CrossRef]
9. Ji, H.; Yu, W.; Hu, X. Influence of load on resonance frequency and resonance impedance of an ultrasonic cutting acoustic system. *J. Vib. Shock* **2016**, *35*, 136–141. (In Chinese)
10. Wang, H.; Zhao, Y.; Ma, X.; Wang, H. Optimal design of constant-stress accelerated degradation tests using the M-optimality criterion. *Reliab. Eng. Syst. Saf.* **2017**, *164*, 45–54. [CrossRef]
11. Xu, J.; Yue, Q.; Zha, H.; Yuan, X.; Cai, X.; Xu, C.; Xu, C.; Ma, Y.; Feng, P.; Feng, F. Wear reduction by toughness enhancement of disc tool in Nomex honeycomb composites machining. *Tribol. Int.* **2023**, *185*, 108475. [CrossRef]
12. Liyang, K. Research on Theoretical Model of Ultrasonic Power Energy Transfer. Master's Thesis, Hangzhou Dianzi University, Hangzhou, China, 2019.
13. Sindhu, T.N.; Atangana, A. Reliability analysis incorporating exponentiated inverse Weibull distribution and inverse power law. *Qual. Reliab. Eng. Int.* **2021**, *37*, 2399–2422. [CrossRef]
14. Wooldridge, J.M. *Introductory Econometrics A Modern Approach*, 7th ed.; Tsinghua University Press: Beijing, China, 2022; pp. 96–99.
15. Roshan, S.; Mohan, B.R.; Kumar, M.; Vandanapu, N. Model selection among log-normal, Weibull, Gamma and generalized exponential distributions. In Proceedings of the 2017 6th International Conference on Reliability, Infocom Technologies and Optimization (Trends and Future Directions)(ICRITO), Noida, India, 20–22 September 2017.
16. Liu, C.J. Accelerated Life Test and Life Evaluation of Semiconductor Lighting. Master's Thesis, Nanchang University, Nanchang, China, 2016.
17. Tang, X.S.; Li, D.Q.; Zhou, C.B.; Phoon, K.K.; Zhang, L.M. Impact of copulas for modeling bivariate distributions on system reliability. *Struct. Saf.* **2013**, *44*, 80–90. [CrossRef]
18. Liu, W.; Shao, Y.; Li, C.; Li, C.; Jiang, Z. Development of a Non-Gaussian Copula Bayesian Network for Safety Assessment of Metro Tunnel Maintenance. *Reliab. Eng. Syst. Saf.* **2023**, *238*, 109423. [CrossRef]
19. Zhang, J.; Gao, K.; Li, Y.; Zhang, Q. Maximum Likelihood Estimation Methods for Copula Models. *Comput. Econ.* **2022**, *60*, 99–124. [CrossRef]
20. Pan, Y.; Zhang, L.; Wu, X.; Qin, W.; Skibniewski, M.J. Modeling face reliability in tunneling: A copula approach. *Comput. Geotech.* **2019**, *109*, 272–286. [CrossRef]